Cover Page

Universiteit Leiden

Author: Fayolle, Edith Carine
Title: From ice to gas : constraining the desorption processes of interstellar ices
Issue Date: 2013-10-01

6

Indirect UV photodesorption from CO:N_2 binary ices - an efficient grain-gas process -

Abstract. UV ice photodesorption is an important non-thermal desorption pathway in many interstellar environments that has been invoked to explain observations of cold molecules in disks, clouds and cloud cores. Systematic laboratory studies of the photodesorption rates, between 7 and 14 eV, from CO:N_2 binary ices, have been performed at the DESIRS vacuum UV beamline of the synchrotron facility SOLEIL. The photodesorption spectral analysis demonstrates that the photodesorption process is indirect, i.e. the desorption is induced by a photon absorption in sub-surface molecular layers, while only surface molecules are actually desorbing. The photodesorption spectra of CO and N_2 in binary ices therefore depend on the absorption spectra of the dominant species in the sub-surface ice layer, which implies that the photodesorption efficiency and energy dependence are dramatically different for mixed and layered ices compared to pure ices. In particular, a thin (1-2 ML) N_2 ice layer on top of CO will effectively quench CO photodesorption, while enhancing N_2 photodesorption by a factors of a few (compared to the pure ices) when the ice is exposed to a typical dark cloud UV field, which may help to explain the different distributions of CO and N_2H^+ in molecular cloud cores. This indirect photodesorption mechanism may also explain observations of small amounts of complex organics in cold interstellar environments.

M. Bertin, E. C. Fayolle, C. Romanzin, H. A. M. Poderoso, X. Michaut, L. Philippe,
P. Jeseck, K. I. Öberg, H. Linnartz and J.-H. Fillion,
submitted to the Astrophysical Journal

6.1 Introduction

In cold and dense regions of the interstellar medium (ISM), characteristic of star and planet formation, gaseous atoms and molecules stick onto dust grains forming ice mantles in relatively short time scales. At these very low temperatures (< 20 K), thermal desorption is negligible for all molecules except H$_2$. Yet, molecules are detected in the gas phase for temperatures below their condensation temperature and this implies the existence of efficient non-thermal desorption processes. These comprise desorption induced by cosmic rays, chemically-induced desorption and vacuum UV photodesorption. The latter has been proposed as an important desorption pathway, particularly in the surface layers of proto-planetary disks (Willacy & Langer 2000; Dominik et al. 2005; Hogerheijde et al. 2011). It may also account for the gas-to-ice abundance ratio for a number of species as observed in other dense regions of the ISM (Coutens et al. 2012; Hollenbach et al. 2008), including the edges of molecular clouds where external UV photons can alter the ice mantle formation, or in the inner part of dense molecular clouds where UV photons are produced by the cosmic-ray ionization of H$_2$ (Caselli et al. 2012). Photodesorption, therefore, is of general importance, influencing the chemistry at different locations in denser regions in space.

Quantitative photodesorption yields from low temperature ices were first obtained experimentally for H$_2$O (Westley et al. 1995a,b). Over the last five to seven years photodesorption rates have been determined for other pure ice samples using broad band, hydrogen discharge lamps; CO (Öberg et al. 2007; Muñoz Caro et al. 2010), H$_2$O/D$_2$O (Öberg et al. 2009b), N$_2$ and CO$_2$ (Öberg et al. 2009; Bahr & Baragiola 2012; Yuan & Yates 2013), O$_2$ and O$_3$ (Zhen et al, submitted). Molecular dynamics calculations have been performed for water ice (Andersson et al. 2006, 2005; Arasa et al. 2010, 2011) and are in good agreement with the experimental findings. More recently, wavelength-specific studies have been performed and for CO, N$_2$ and O$_2$ absolute photodesorption rates have been determined between 7 and 14 eV (Fayolle et al. 2011, Fayolle et al in press). The spectral dependence of the photodesorption yield is of fundamental interest for modeling regions in space with different spectral energy distributions. Moreover, this approach has been very successful to link the photodesorption process in the ice to the solid state mechanisms at play, highlighting the physical-chemical parameters governing the photodesorption process. In the case of CO and N$_2$ the wavelength dependent intensity of the measured Photon-Stimulated Desorption signals (PSD) follows directly the electronic transitions in the condensed molecules(Fayolle et al. 2011, Fayolle et al in press). This is a signature of a mechanism known as DIET (desorption induced by electronic transition), not (substantially) involving dissociation/recombination in the ices. An even more detailed picture of the involved surface processes has been derived from the investigation of layered ^{13}CO/^{12}CO films (Bertin et al. 2012) showing that the photodesorption is mediated by the ice lattice. This study pointed out a sub-surface excitation mechanism in which electronically excited molecules release their energy through intermolecular vibrational motion into a desorption channel. Recently, Yuan & Yates (2013) addressed the crucial role of this energy transfer from the ice lattice by comparing Lyman-α photodesorption at 75 K for pure ^{12}CO$_2$, pure ^{13}CO$_2$ and $^{12/13}$CO$_2$ mixed ices.

In the present work we go one step further and study the photodesorption efficiency of a binary ice mixture made of different chemical species. We present wavelength dependent photodesorption measurements from CO and N_2 binary ices (layered and mixed) at 10 K. This is interesting from a physical-chemical point of view; their masses are nearly equivalent, their photodesorption mechanisms are similar and their binding energies to the solid are comparable, but the two molecules have strong, non-coinciding photodesorption features in the VUV (around 8.5 and above 12.3 eV for CO and N_2, respectively) in their pure solid phase. The choice for a CO:N_2 ice is particularly relevant from an astronomical point of view. CO is highly abundant, both in the gas phase and in the solid state, representing the main molecular component after H_2. Molecular nitrogen, N_2, is not directly detectable due to its lack of a permanent dipole moment, but is considered as one of the main reservoir of nitrogen in the gas phase, due to its high stability. Its presence in the ISM is evidenced by the detection of N_2H^+ resulting from a proton transfer reaction involving H_3^+ (Bergin et al. 2002; Flower et al. 2006; Hily-Blant et al. 2010). Moreover, N_2 stands at the origin of other processes leading to the formation of more complex N-bearing molecules (Persson et al. 2010, 2012; Hily-Blant et al. 2013). As both CO and N_2 are highly volatile, with accretion temperatures in the 16-20 K regime under ISM conditions and sticking coefficients close to unity, they are the last species to freeze onto dust grains, generating a top layer that can be considered as a binary interstellar ice (Öberg et al. 2005; Bisschop et al. 2006). Nevertheless, observational studies of N_2H^+ and other N-containing species in dense cores indicates that N_2 depletion onto the grains occurs later, i.e. at higher density, than for CO (Bergin et al. 2002; Pagani et al. 2005, 2012). Therefore, it has been suggested that a mechanism leads to a continuous enrichment of gas phase N_2, counterbalancing its accretion on the grains. Chemistry involving CN + N reactions, constantly forming N_2 in the gas, is invoked (Hily-Blant et al. 2010), but, photodesorption processes, preferentially ejecting N_2 instead of CO in the gas phase from a condensed mixture of N_2 and CO, may be an equally important channel.

In this chapter, a laboratory based study of vacuum UV irradiated CO:N_2 binary ice samples as a function of the wavelength is presented. This approach follows successful experiments on pure CO, N_2 and O_2 ice (Fayolle et al. 2011, Fayolle et al in press). In the next section experimental details are given. The results are presented in section 3 and are discussed from a physical-chemical and an astrophysical point of view in section 4.

6.2   Experimental methods

The photodesorption studies are realized in the SPICES (Surface Processes & ICES) setup of the UPMC (Université Pierre et Marie Curie), under ultrahigh vacuum (UHV) conditions (P $\sim$ 1×10^{-10} Torr). The substrate on which ices are grown is a Highly Oriented Polycrystalline Graphite (HOPG) surface. It is mounted on the tip of a turnable cold head that can be cooled down to $\sim$ 10 K by means of a closed cycle helium cryostat. The ice layers are grown in-situ by exposing the cold HOPG substrate to a partial pressure of CO and/or N_2 gases. A dosing tube, placed 1 mm in front of the substrate, allows a local exposure of the gases onto the cold sample without contami-

nating the whole UHV chamber. The isotopologues ^{13}CO (Eurisotop, 99.6 % ^{13}C) and ^{15}N$_2$ (Eurisotop, 97 % ^{15}N) are used in order for them to be distinguishable by mass spectrometry. The quantities of molecules deposited on the substrate are expressed in ML$_{eq}$ (monolayer equivalent) corresponding to the surface density of a compact molecular layer on a flat surface, with 1 ML$_{eq} \approx 1 \times 10^{15}$ molecule.cm^{-2}. Temperature Programmed Desorption (TPD) is used for the calibration of the ice thicknesses, resulting in reproducible parameters for the growth conditions with a precision better than 1 ML$_{eq}$.
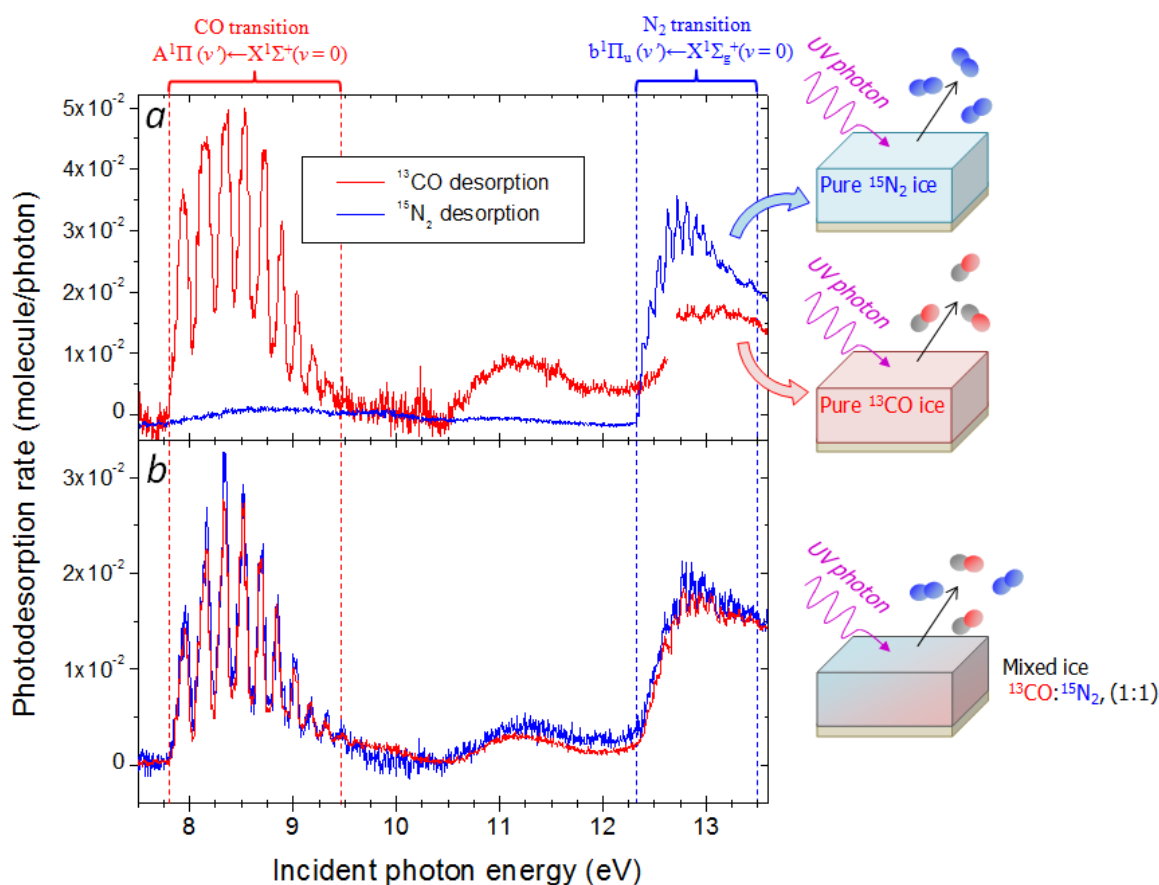

Figure 6.1: Photon-Stimulated Desorption (PSD) spectra of ^{13}CO (red) and ^{15}N$_2$ (blue) from 30 ML of pure ^{13}CO and ^{15}N$_2$ ices (a), and from a mixed ^{13}CO:^{15}N$_2$ ice, in proportion 1:1 (b). The electronic transitions in condensed CO and N$_2$ associated with the main photodesorption features are indicated. All spectra have been obtained for ices kept at 15 K and deposited on HOPG.

.

UV photodesorption is induced through irradiation of the ice sample by the continuous output of the undulator-based vacuum UV DESIRS beamline of the synchrotron SOLEIL (Nahon et al. 2012), providing photons with an energy that can be continuously scanned over the 7 - 14 eV range. A narrow bandwidth of typically 40 meV is selected by the 6.65 m normal incidence monochromator that is implemented on the

beamline. A gas filter in the beamline suppresses the harmonics of the undulator that can be transmitted in higher diffraction orders of the grating. The absolute incident photon flux per surface unit impinging onto the sample is measured by a calibrated photodiode and varies for a given spectral bandwidth of 40 meV between 0.3 and 1.1×10^{13} photons.s^{-1}.cm^{-2} depending on the photon energy. In order to prevent radiation cut-off, the DESIRS beamline is directly connected to SPICES, i.e., without any window.
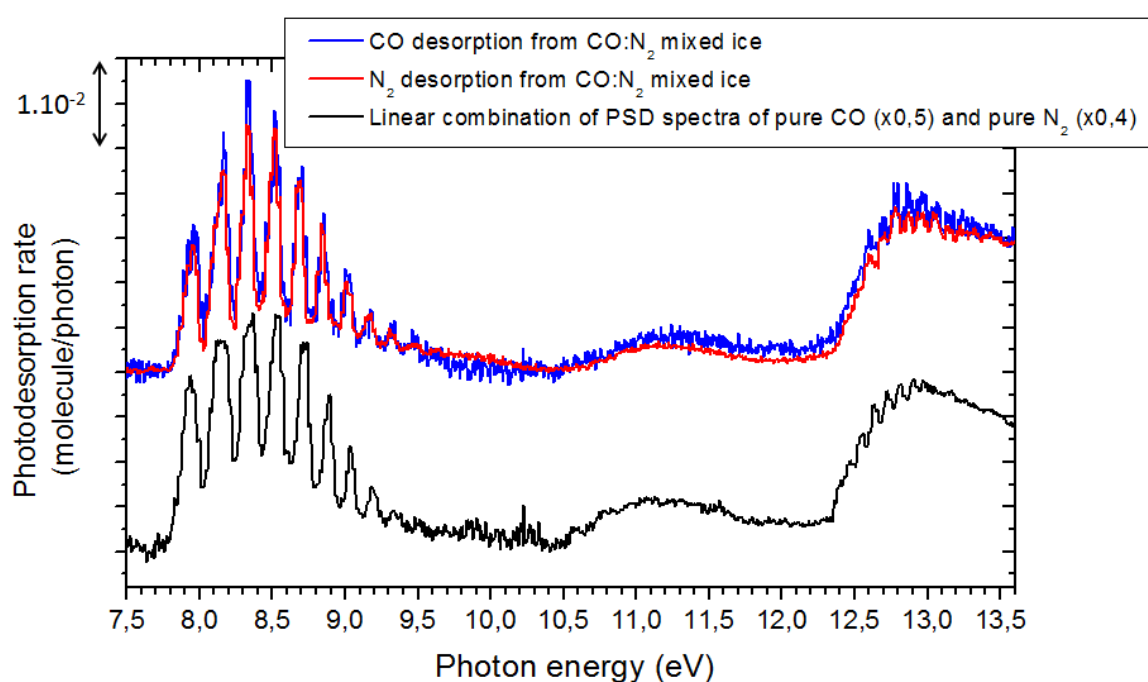

Figure 6.2: Photon-stimulated spectra of N_2 and CO from a mixed CO:N_2 ice, in proportion 1:1, compared with a linear combination of PSD spectra obtained from pure CO ice ($\times$ 0.5) and pure N_2 ice ($\times$ 0.4). The spectra have been acquired from ices deposited on HOPG kept at 15 K.

.

Photon-stimulated desorption spectra, are recorded in real time during ice irradiation, monitoring the gas phase composition upon evaporation by means of a Quadrupole Mass Spectrometer (QMS), as a function of the incident photon energy. In the presented PSD spectra, the photon energy is automatically scanned from 7 to 14 eV with steps of 25 meV. Each energy step lasts $\sim$ 5 s. In parallel, the QMS signal is recorded with a dwell of 1 s, which makes an average of 5 points per energy step. Caution has been taken to ensure that for each data point the 1 s accumulation time is substantially longer than the QMS mass signal build-up time, preventing eventual artifacts due to fast wavelength scanning. The mass resolution of the QMS, as taken

from the Full-Width-at-Half-Maximum (FWHM) of the Gaussian mass peaks associated with ^{13}CO (m = 29 amu) and ^{15}N$_2$ (m = 30 amu) is ~ 0.3 amu. It therefore allows for a fine separation of ^{13}CO and ^{15}N$_2$ signals with negligible overlap. The energy-dependent desorption rate per incident photon is derived from the PSD spectra and the measured energy-dependent photon flux, following the methods described in detail previously (Fayolle et al. 2011, Fayolle et al in press). Additional information on the composition of the condensed phase can also be obtained by monitoring simultaneously Reflection-Absorption-Infrared Spectra (RAIRS) using a Fourier transform infrared (FT-IR) spectrometer.

6.3   Results

Figure 6.1a shows PSD spectra obtained upon VUV irradiation of the pure ^{13}CO and ^{15}N$_2$ ices. These spectra have already been presented and discussed in previous studies. The photodesorption rates exhibit energy-dependent efficiencies that follow closely the VUV absorption of the pure molecular solids, with patterns that are associated with electronic transitions of the condensed molecules. For instance, the features observed between 7.9 and 9.5 eV in the CO PSD spectrum are due to vibronic bands in the $A^1\Pi - X^1\Sigma^+$(v',0) electronic transition, each peak being associated with a transition towards a vibrational sub-level v' in the A-state of solid ^{13}CO (Fayolle et al. 2011). In a similar way, the main feature responsible for the photodesorption of solid ^{15}N$_2$ (above 12.3 eV) is associated with the $b^1\Pi_u - X^1\Sigma_g^+$(v',0) transition in pure nitrogen ice (Fayolle et al., in press). The observation of such structures in the energy-resolved photodesorption rates is a clear signature for a DIET mechanism, as discussed in (Fayolle et al. 2011, Fayolle et al in press). It has been shown that the excitation mainly takes place in a subsurface region of the ice (2-3 upper molecular layers), while only the molecules from the topmost layer are ejected into the gas phase. A short-range energy transfer from the excited to the desorbing molecules is therefore expected to occur, presumably through the coupling between the relaxation of the excited species and the excitation of intermolecular collective vibrational modes (Bertin et al. 2012). It should be noted that the thickness of our samples is less than the photon penetration depth, implying that photons can excite molecules deeper within the ice and even reach the graphite substrate. However, according to (Bertin et al. 2012), neither the substrate nor underlying layers are contributing to the desorption features observed here. The question that is addressed here is how these properties translate in a mixed ice, consisting of both CO and N$_2$.

6.3.1   Photodesorption from mixed CO:N$_2$ ice

Figure 6.1b displays the PSD spectra for both ^{13}CO and ^{15}N$_2$ desorbing upon VUV irradiation of an ice grown from a 1:1 CO:N$_2$ mixture. There is a clear difference between the results for the pure and mixed ice irradiation. As discussed above, the pure ice spectra are very different, whereas, for the mixed ice, the PSD spectra are identical. A comparison with Fig. 6.1a shows that the photodesorption spectra of the CO:N$_2$ ice mixture results in a superposition of the PSD spectra of the two pure constituents.

The ejection of any surface molecule in the mixed ice, clearly, is initiated by the electronic excitation of any other molecule. In particular, the PSD spectra of the mixed ice show that the excitation of solid CO into its $A^1\Pi$ state leads to the desorption of surface N_2 (7.9 - 9.5 eV), and that solid N_2 excitation into its $b^1\Pi_u$ state initiates CO desorption above 12.3 eV. This finding is fully consistent with the previously introduced concept of an indirect DIET mechanism; part of the excess energy deposited in the ice by the vacuum UV photon absorption is transferred from one to the other molecule independently of its chemical nature - causing desorption. Within this respect, the process shows similarities with the *indirect adsorbate-mediated photodesorption* proposed by Thrower et al. (2008) in which the energy of a laser pulse absorbed by benzene molecules is transferred to water molecules enhancing their desorption.

For a given energy, the absolute photodesorption rates of CO and N_2 from the mixed ice are lower by a factor of 2 than the corresponding value derived for the pure ices. In fact, the PSD spectra of the mixture can be fitted with a very good agreement by a linear combination of the desorption spectra of pure $^{15}N_2$ and pure ^{13}CO in which each constituent contributes to about ~ 0.5 of the overall desorption signal (Fig. 6.2). As the surface of the mixed film is expected to be composed of half CO and half N_2 molecules, and as the adsorption energies of CO and N_2 are very close (Bisschop et al. 2006), this shows that the amount and efficiency of the energy transfer to surface molecules upon subsurface CO excitation or N_2 excitation are about the same.

6.3.2 Photodesorption from layered N_2/CO and CO/N_2 ices

Photon-stimulated desorption spectra of ^{13}CO (left panel) and $^{15}N_2$ (right panel) obtained from a pure 25 ML_{eq} ^{13}CO ice covered by an increasing layer of $^{15}N_2$ are shown in Fig. 6.3. In the case of pure CO or N_2 ice (top left and bottom right, respectively) the characteristic desorption profiles around 8.5 and above 12.3 eV are seen. When the CO ice is covered by 0.9 ML_{eq} of N_2, the CO desorption yield drops substantially, and it is almost entirely suppressed above ML_{eq}. This behavior, also observed in the case of layered $^{13}CO/^{12}CO$ (Bertin et al. 2012), shows that mostly the surface molecules are susceptible to desorb upon UV irradiation.

When investigating the PSD of $^{15}N_2$ for a low thickness of N_2 overlayer (0.9 ML_{eq}), one can see that its photodesorption pattern mimicks almost completely the one of the pure CO ice, demonstrating that its photodesorption is triggered only by the absorption of the underlying CO molecules. In particular, its photodesorption in the 7.9 - 9.5 eV range, associated with the excitation of the $A^1\Pi$ state of solid CO, becomes the dominant contribution, although pure solid N_2 does not photodesorb at these energies. In contrast, photodesorption initiated by the N_2 excitation in the $b^1\Pi_u$ state ($>$ 12.3 eV) is not clearly observed. The adsorption of a small quantity of N_2 onto a CO ice therefore drastically modifies the energy-dependence of its photodesorption process. For increasing thickness of the $^{15}N_2$ overlayer, the N_2 excitation contribution to the N_2 PSD spectra gradually recovers the one of the pure N_2 ice. The contribution of the CO excitation becomes very weak for N_2 thicknesses above ML_{eq}, showing that the range for an efficient energy transfer involves less than 3 molecular layers.

Figure 6.4 shows the results of layered experiments in which 25 ML_{eq} $^{15}N_2$ ice is
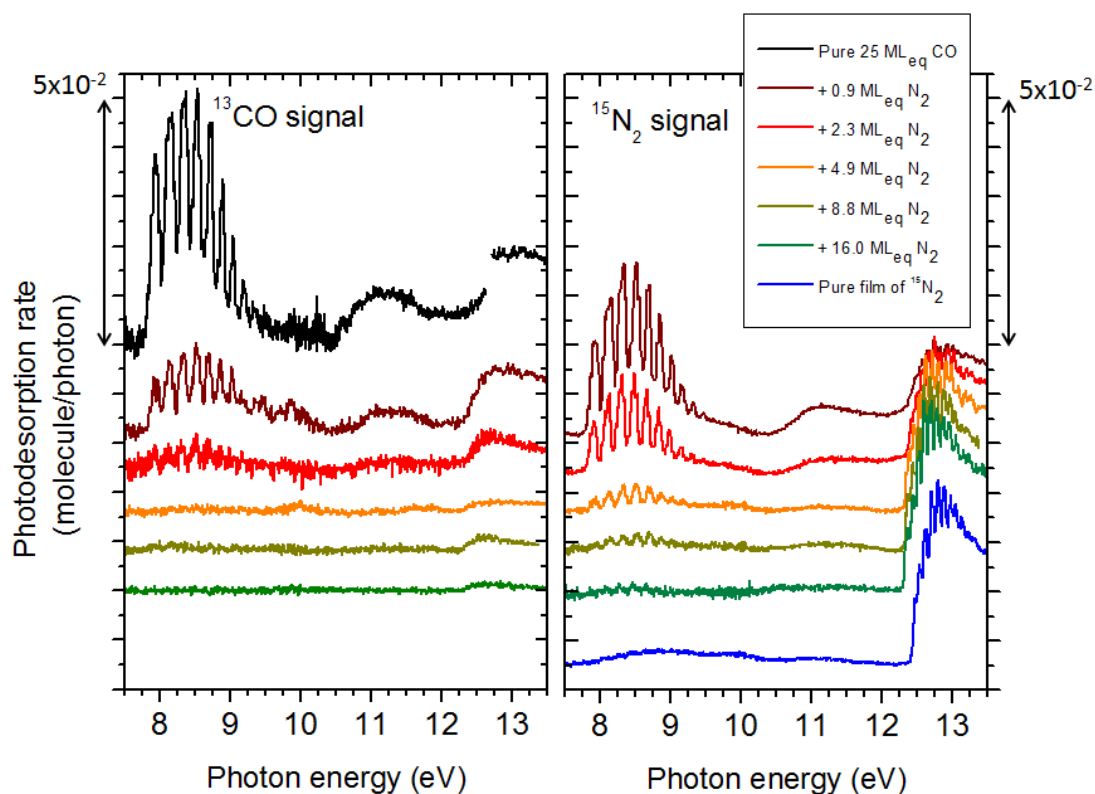
Figure 6.3: Photon-stimulated desorption spectra of ^{13}CO (left) and ^{15}N$_2$ (right) from 25 ML$_{eq}$ of ^{13}CO ice covered by an increasing ^{15}N$_2$ layer on top. The PSD spectrum obtained from a pure 25 ML$_{eq}$ ^{15}N$_2$ ice is also presented for comparison. All spectra are recorded for 15 K ices, deposited on HOPG.

.

covered by an increasing layer of ^{13}CO. The experiment is essentially identical to the previous one (fig. 6.3), but the role of N$_2$ and CO are exchanged. The N$_2$ photodesorption signal vanishes for a larger CO coverage and a clear vibrational progression in the ^{13}CO desorption channel is found that corresponds to an excitation into the $b^1\Pi_u$ state of N$_2$. This feature is superimposed over a continuous desorption of ^{13}CO observed above 12.5 eV in pure CO samples (Fayolle et al. 2011). As for the 25 ML$_{eq}$ ^{13}CO ice covered by ^{15}N$_2$ the spectra are fully consistent with a process in which only surface molecules desorb after excitation of sub-surface species.

6.4 Discussion and astrophysical implications

6.4.1 Role of ice structure and composition on absolute photodesorption rates

The VUV photodesorption of coadsorbed N$_2$ and CO presents very different energy-dependent profiles and efficiencies compared to pure N$_2$ and CO ices. Both molecules mainly desorb through an indirect mechanism, where the excitation of a subsurface
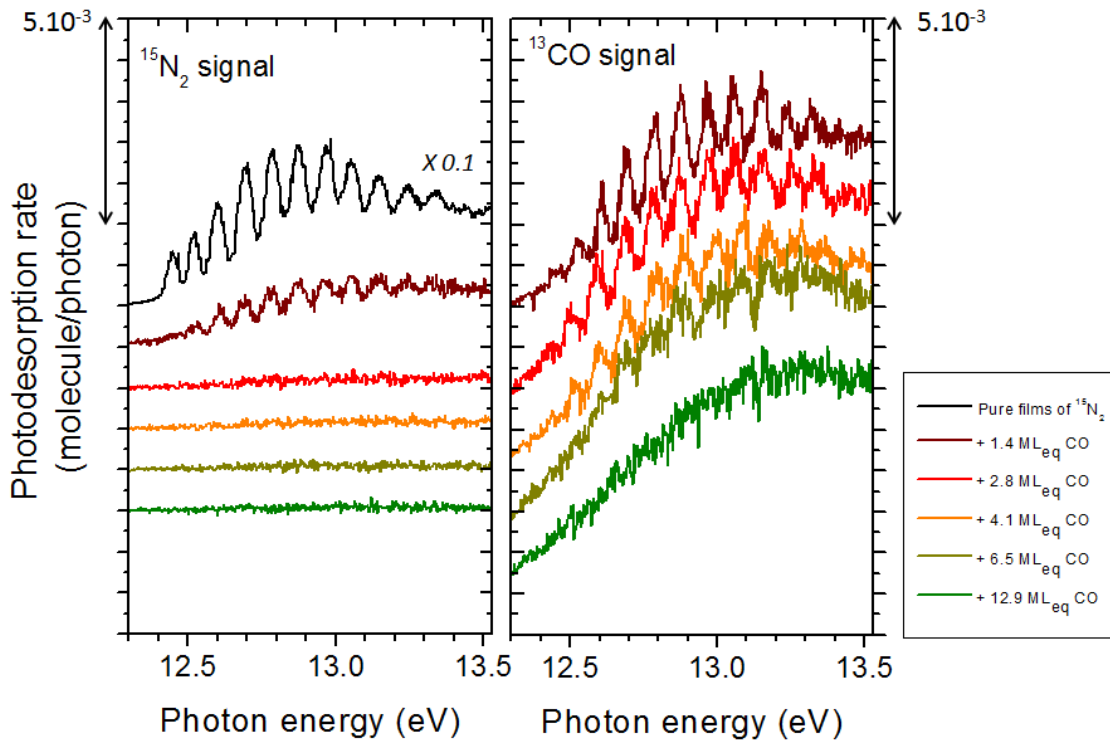
Figure 6.4: Photon-stimulated desorption spectra of $^{15}N_2$ (left) and ^{13}CO (right) from 25 ML_{eq} of $^{15}N_2$ ice covered by an increasing layer of ^{13}CO ice on top. All spectra are recorded for 15 K ices, deposited on HOPG.

.

molecule, whether CO or N_2, leads to the desorption of N_2 and CO surface molecules. Because this indirect mechanism involves energy transfer from the excited molecule to the desorbing one, presumably by collective vibrational mode excitation, the photodesorption energy-dependence and efficiency depend strongly on the nature of the intermolecular interactions. In general intermolecular interactions in solids may promote the photodesorption, but also quench it. This has been demonstrated for CO_2 in interaction with other isotopologues or rare gas matrices (Yuan & Yates 2013), and for CO in interaction with H_2O ice (Bertin et al. 2012). For the latter case, an explanation has been proposed, stating that the photodesorption efficiency is driven by the competition between two excess energy relaxation pathways: (*i*) relaxation by intermolecular phonon modes of the ice, coupled to desorption and (*ii*) relaxation by transfer to intramolecular vibration modes of neighboring molecules. If the first relaxation pathway is dominant, the photodesorption will be efficiently triggered by UV absorption of neighboring molecule. If the latter pathway dominates the relaxation process, as it is the case when excited CO transfers efficiently its excess energy to the O-H dangling bond vibrations of neighboring water molecules, then the photodesorption gets hindered. In both cases, the constructive and destructive matrix effects are a consequence

Table 6.1: Energy-integrated photodesorption rates of CO and N$_2$ in several regions of the ISM for pure ices, mixed CO:N$_2$ ices in a proportion of 1:1, and 0.9 monolayer equivalent (ML$_{eq}$) of N$_2$ deposited on top of a CO ice. The rates are for ices kept at 15 K. All values are given in desorbed molecules per incident photon.

Environment	Pure CO ice[a]	Pure N$_2$ ice[b]	CO from Mixture CO:N$_2$ 1:1	CO from 0.9 ML$_{eq}$ N$_2$ on CO	N$_2$ from Mixture CO:N$_2$ 1:1	N$_2$ from 0.9 ML$_{eq}$ N$_2$ on CO
Edges of clouds[a]	1.3×10^{-2}	2.6×10^{-3}	5.7×10^{-3}	5.3×10^{-3}	5.5×10^{-3}	8.0×10^{-3}
Prestellar cores[b]	1.0×10^{-2}	2.2×10^{-3}	3.0×10^{-3}	3.9×10^{-3}	3.0×10^{-3}	5.1×10^{-3}
Protoplanetary disk[c]	7.2×10^{-2}	5.3×10^{-3}	2.3×10^{-3}	3.0×10^{-3}	2.1×10^{-3}	2.7×10^{-3}

Note. — Using UV field from [a]Mathis et al. (1983), [b]Gredel et al. (1987), [c]Herczeg et al. (2002); Valenti et al. (2003); Johns Krull & Herczeg (2007). [d] and [e] are values from Fayolle et al. (2011) and Fayolle et al. (in press) respectively

of the indirect character of the photodesorption mechanism.

Because the intermolecular coupling in the ice between excited and surface molecules can drastically modify the photodesorption process, it is expected that different composition, but also different structure of the ice, will modify the energy-integrated photodesorption yield for a given UV field. This is illustrated for the N$_2$/CO binary ices. As shown in Figs. 1 and 3, coadsorption of N$_2$ with CO promotes N$_2$ desorption in the 7 - 11.5 eV range whereas it decreases the desorption efficiency of CO in the same energy range. To quantify this effect, energy-integrated photodesorption rates have been derived from our PSD curves for three types of interstellar vacuum UV profiles as a function of the CO:N$_2$ layered/mixed ices composition. The results are displayed in Table 1. To obtain these values, our energy-resolved desorption rates have been convoluted with vacuum UV profiles describing the interstellar radiation field (ISRF) at the edge of clouds (Mathis et al. 1983), the effect of secondary photons from cosmic ray impacts in dense cores (Gredel et al. 1987), and a TW Hydræ radiation field as model for the UV field in proto-planetary disks (Herczeg et al. 2002; Valenti et al. 2003; Johns Krull & Herczeg 2007). The resulting photodesorption rates are varying depending on (*i*) the UV field considered, (*ii*) the ice composition and (*iii*) the internal ice organization (layered versus mixed). Compared to pure ices the photodesorption rates from the binary ices change by up to an order of magnitude. The general trend is to decrease the CO photodesorption rate from $> 1 \times 10^{-2}$ to 2-6 $\times 10^{-3}$ molecules.photon^{-1}, and to increase the N$_2$ photodesorption rate by a factor of 2-3. This shows that a proper description of the VUV photodesorption process has to take into consideration the structure and composition of the ice on which the molecules are adsorbed; the photodesorption rates extracted from pure molecular solids may not be realistic in the case of more complex ices, as typically present in the interstellar medium.

6.4.2   Implications for N_2 and CO gas phase abundance in dense cores

In dense cores, non-thermal desorption, including photodesorption, is constantly enriching the gas phase, competing with gaseous species freezing-out on the grains. Thus a variation of the photodesorption rate with chemical composition and ice morphology directly influences the steady state between the two processes. The details of the processes that determine the steady-state are especially important for N_2 because of the longstanding question why N_2 molecules remain (partially) in the gas-phase in cold interstellar regions where CO is found to be completely frozen out on grain surfaces (Bergin et al. 2002; Pagani et al. 2012). This cannot be explained by thermal processes alone, since N_2 and CO are expected to condense on icy grains less than 2 K apart, and with the same efficiency (Öberg et al. 2005; Bisschop et al. 2006). The photodesorption rates as extracted from pure CO and N_2 ices are not resolving the issue either since the photodesorption rate is substantially lower for pure N_2 than for pure CO for realistic dark cloud UV fields (Table 6.1). However, considering pure ices may be inappropriate, as discussed in section 4.1, since the ice structure and composition may impact the CO and N_2 photodesorption rates.

Since CO and N_2 are expected to freeze-out in the same temperature range, it is rather unlikely that the top layers of the ices are composed of solely pure N_2 or pure CO thick layers. Instead, we expect that both species are coadsorbed at the surface of the icy grains. The exact nature of the top layers depends on the abundance of N_2 as compared to CO, as well as on the proximity in time and space of CO and N_2 freeze-out. The amount of N_2 being relatively low compared to CO (Bergin et al. 2002; Maret et al. 2006), it is expected that solid N_2 is frozen on or into a CO-rich environment. Whether the outer layers of the grain will be layered or mixed is not that easy to answer, and is likely source-dependent. N_2 is expected to condense for 2 K lower temperatures, compared to CO (Flower et al. 2006; Hily-Blant et al. 2010), which would, for low cooling speed of the cloud, lead to the growth of a thin N_2 layer on top of CO-rich ice. In the case of a shorter cooling time, such a temperature difference would not be sufficient to result in segregated layers, and N_2 would be embedded in a CO matrix.

As explained before, the photodesorption rates extracted from pure CO and pure N_2 in prestellar cores cannot explain the N_2 constant gas phase enrichment in region where CO is totally frozen: the pure N_2 photodesorption is substantially less efficient than for pure CO. If we consider instead a mixed CO:N_2 1:1 ice, the photodesorption rates of CO and N_2 in prestellar cores become identical, as shown on Table 6.1. In the case of a more realistic system, i.e. a small amount (0.9 ML_{eq}) of N_2 on CO ice, then, the CO photodesorption rate strongly decreases, whereas the N_2 photodesorption rate is promoted. Then, the N_2 desorption becomes more efficient than the CO one, and photodesorption can explain gas phase N_2 enrichment. Thus, under interstellar conditions N_2 will be photodesorbed at least as efficiently as CO as long as they are coadsorbed, and in many core environments, the N_2 photodesorption may exceed that of CO providing a natural explanation to why N_2 is maintained longer in the gas phase compared to CO.

6.4.3   Organics desorption through CO photoexcitation?

The indirect nature of the photodesorption process may have more general implications beyond the explanation of the CO and N$_2$ abundances in the ISM. The ability of CO ice to transfer part of the absorbed energy to a surrounding molecule may act as an important indirect photodesorption channel of other species as well, and in particular of formaldehyde H$_2$CO, methanol CH$_3$OH, and possibly more complex organic molecules, providing a non-dissociative non-thermal desorption pathway. Indeed, these species are expected to form into the CO-rich icy mantles, by hydrogenation processes (Watanabe & Kouchi 2002; Fuchs et al. 2009; Herbst & van Dishoeck 2009; Taquet et al. 2013). Moreover, in (Cuppen et al. 2011), it was spectroscopically shown that interstellar CO ice gets intimately mixed with methanol and that the outer CO layer of the ice is essentially water free.

Organic molecules are expected to efficiently photodissociate upon UV photon irradiation, as it the case for instance for CH$_3$OH (Öberg et al. 2009a), leading to the formation of photoproducts that can eventually desorb. Photochemistry in the ice represents an important decay channel upon UV excitation and is in direct competition with the photodesorption of the intact molecule. When the photodestruction is dominating, it can even prevent the intact molecule to be ejected in the gas phase, making the photodesorption decay channel totally inactive. Embedded in a CO-rich environment, however, such molecules may react differently under UV irradiation: even when the direct UV absorption of organics leads to their destruction, a photon absorption by the surrounding and more numerous CO molecules could lead to the desorption of the surface-located organics via a similar mechanism as highlighted for CO:N$_2$. The CO would then act as a 'seed' for intact molecular photodesorption, preventing their destruction in the ices and thus enriching the gas phase with small organics. Such a process could then explain the observed gas abundances of organics, observed in the cold regions of the ISM (Öberg et al. 2010; Bacmann et al. 2012; Tercero et al. 2013). Whether this indirect photodesorption process can be generalized to heavier and more strongly bound species than CO and N$_2$ needs to be experimentally verified, however.

6.5   Summary and conclusions

From a systematic set of energy (7 - 14 eV) resolved (40 meV) photodesorption laboratory studies on CO:N$_2$ binary ices, both mixed and layered the following conclusions can be made:

– The desorption is induced by a photon absorption in the topmost molecular layers, while only surface molecules are actually desorbing. This implies an energy transfer from the subsurface excited molecule to the surface ones. Thus, the photodesorption rate is not linked to the absorption spectrum of the desorbing molecule, but is instead associated to the absorption profile of the surrounding species, located deeper in the ice. When N$_2$ and CO are mixed in equal proportions, their photodesorption spectra become superimposable, and reflect a linear combination of the photodesorption spectra of both pure ices. When a small quantity of N$_2$ is deposited at the surface of a CO ice, then, its photodesorption spectrum reflects mostly the one of

pure CO. This is remarkable since, in this case, the N_2 major desorption feature lies in the 7.9 - 9.5 eV energy range, in which pure solid N_2 does not absorb.

– This indirect desorption mechanism and its dependence on ice structure and wavelength influence the (overall) desorption efficiency in space. Considering the range of indirect photodesorption processes, we suggest that the photodesorption rates experimentally obtained from pure ices should only be used for molecules which can form pure phases in the ISM ices, exceeding at least two to three molecular toplayers, as it may be the case for CO in some cold regions. Below this thickness, or when molecules are mixed with others, photodesorption rates obtained from a more realistic composite ice should lead to a more accurate description of the non-thermal desorption. Here both chemical composition and molecular organization play a role.

– The results presented here provide a way to replenish nitrogen in the prestellar cores, contributing to the unexplained low depletion rate of N_2 as compared to CO. If the rates derived for pure CO and N_2 are used, CO should desorb with an efficiency that is almost one order of magnitude higher than for N_2. This is not in agreement with observations concluding that gaseous CO depletes on the grains with a higher rate than N_2. When considering the rates extracted from a more realistic system, most probably a layered N_2/CO structure with a small amount of N_2, as presented here, gaseous N_2 will be enriched with respect to CO. A detailed astrochemical modeling is required to quantify the extent of this N_2 enrichment.

– Finally, the mechanism introduced here may explain observation of organic species in the gas phase in very cold environments of space. Indirect photodesorption could indeed result in the release of gas phase intact organic species by UV absorption of neighboring molecules, whereas direct UV photo-excitation of this species may lead to its destruction through photolysis.